

H₄: A Challenging System For Natural Orbital Functional Approximations

Eloy Ramos-Cordoba,¹ Xabier Lopez,¹ Mario Piris,^{1,2} and Eduard Matito^{1,2}

¹*Faculty of Chemistry, University of the Basque Country UPV/EHU, and Donostia International Physics Center (DIPC), P.K. 1072, 20080 Donostia, Euskadi, Spain^a*

²*IKERBASQUE, Basque Foundation for Science, 48011 Bilbao, Spain*

(Dated: 5 March 2022)

The correct description of nondynamic correlation by electronic structure methods not belonging to the multireference family is a challenging issue. The transition of D_{2h} to D_{4h} symmetry in H₄ molecule is among the most simple archetypal examples to illustrate the consequences of missing nondynamic correlation effects. The resurgence of interest in density matrix functional methods has brought several new methods including the family of Piris Natural Orbital Functionals (PNOF). In this work we compare PNOF5 and PNOF6, which include nondynamic electron correlation effects to some extent, with other standard *ab initio* methods in the H₄ D_{4h}/D_{2h} potential energy surface. Thus far, the wrongful behavior of single-reference methods at the $D_{2h} - D_{4h}$ transition of H₄ has been attributed to wrong account of nondynamic correlation effects, whereas in geminal-based approaches it has been assigned to a wrong coupling of spins and the localized nature of the orbitals. We will show that actually *interpair* nondynamic correlation is the key to a cusp-free qualitatively correct description of H₄ PES. By introducing *interpair* nondynamic correlation, PNOF6 is shown to avoid cusps and provide the correct smooth PES features at distances close to the equilibrium, total and local spin properties along with the correct electron delocalization, as reflected by natural orbitals and multicenter delocalization indices.

I. INTRODUCTION

The correct description of nondynamic correlation effects is a challenging task for electronic structure methods. In wave function approaches, a multireference ansatz is needed to properly account for these effects. The computational scaling cost of such methods limits their use to systems of moderate size. Within density functional theory (DFT) the proper inclusion of nondynamic correlation effects is an open problem.¹ In practice, a broken-symmetry calculation is usually performed producing wrong spin densities.²

An alternative to both wave function and DFT methods is natural orbital functional theory (NOFT).³⁻⁵ In recent years, several functionals have been proposed by reconstruction of the two-particle reduced density matrix (2-RDM) in terms of the one-particle reduced density matrix (1-RDM).⁶ In particular, within the family of Piris Natural Orbital Functionals (PNOF),^{7,8} PNOF5⁹ and PNOF6¹⁰ are among the best candidates to treat nondynamic correlated systems. They describe properly the dissociation limit of several molecules, recovering the correct integer number of electrons on each fragment upon dissociation.^{10,11} Both PNOF5 and PNOF6 belong to the family of orbital-pairing approaches, but the former only includes intrapair electron correlation while in the latter electrons on different pairs are also correlated. The inclusion of interpair electron correlation in PNOF6 allows a better description of correlation effects and it also removes the symmetry-breaking artifacts that are present in independent-pairs approaches such as PNOF5 when treating delocalized systems.¹⁰

The purpose of this manuscript is to analyze the effect of

interpair electron correlation on the treatment of nondynamic correlation by investigating the performance of PNOF5 and PNOF6 and several standard *ab initio* computational methods. To this end we will examine the D_{4h}/D_{2h} potential energy surface of the planar H₄ model (hereafter, simply PES).

H₄ has been extensively used to test single-reference post-Hartree-Fock methods^{2,12-21} and geminal-based theories.^{22,23} Hartree-Fock, MP2 and MP3 show a spurious cusp on the PES of H₄ as the system evolves from D_{2h} to D_{4h} symmetry. The cusp is the maximum energy value along the symmetry transition. Conversely, traditional coupled cluster (CC) methods predict a cusp but this cusp is a local minimum in the $D_{2h} - D_{4h}$ transition. Recently, Bulik *et al.* have shown that an improvement of the description of correlated systems can be also achieved by removing terms in traditional CC theory.² Variational CC approaches also improve this wrong behavior of the traditional CC implementations,^{12,13,19} however, most of these approaches revert the local minimum to a local maximum but most of them do not avoid the presence of a spurious cusp. Geminal-based theories predict a (maximum) cusp at the square geometry. Jeszenszki *et al.*²² have attributed this failure to an insufficient account of spin couplings and the localized character of the orbitals. By including triplet components in the geminals, the orbitals become delocalized and the characteristic cusp vanishes, but the resultant PES is not completely smooth and wave function becomes spin contaminated. The authors also examined the local spin²⁴⁻²⁶ of the system using different geminal-based approaches. Jeszenszki *et al.*²² have found that singlet-coupled geminals fail to describe correctly local spins at the D_{4h} geometry. The inclusion of triplet components improve the results but the local spin values are not smooth along the PES.

Thus far, the wrongful behavior of single-reference methods at the $D_{2h} - D_{4h}$ transition of H₄ has been ascribed to

^aElectronic mail: eloy.raco@gmail.com, ematito@gmail.com

a wrong account of nondynamic correlation effects,^{2,12,13,19} whereas in geminal-based approaches, the spurious (maximum) cusp has been attributed to a wrong coupling of spins and the localized nature of the orbitals.²² We will show that actually *interpair* nondynamic correlation is the key to qualitative cusp-free correct description of H₄ PES. By introducing *interpair* nondynamic correlation, PNOF6 is shown to avoid cusps and provide the correct smooth PES features, total and local spin properties along with the correct electron delocalization, as reflected by natural orbitals and multicenter delocalization indices.

II. THEORY

A. PNOF5/PNOF6

In this section we will briefly review the formulation of PNOF5⁹ and PNOF6.¹⁰ Both PNOF5 and PNOF6 belong to the family of orbital-pairing methods, which divide the spatial orbital space into subspaces (a set of orbitals) that contain two electron each. These methods couple each orbital g below the Fermi level ($F = N/2$, where N is the number of electrons of the system) with N_c orbitals above it, being Ω_g the subspace containing orbital g and its coupled counterparts. The original formulations of both functionals were introduced for $N_c = 1$ but subsequently extended versions ($N_c > 1$) were reported.^{27,28} The sum rule for the occupation numbers (n) is fulfilled for each of the $N/2$ subspaces Ω_g ,

$$\sum_{p \in \Omega_g} n_p = 1 \quad (1)$$

where p denotes a spatial natural orbital (NO) and n_p its occupation number.

The PNOF5 and PNOF6 energy expressions for a singlet state system can be written as

$$E = \sum_{g=1}^F E_g + \sum_{f \neq g} \sum_{p \in \Omega_f} \sum_{q \in \Omega_g} E_{pq}^{int}. \quad (2)$$

The first term of Eq. (2) corresponds to the sum of energies of F independent pairs with energy E_g , namely,

$$E_g = \sum_{p \in \Omega_g} n_p (2\mathcal{H}_{pp} + \mathcal{J}_{pp}) + \sum_{p, q \in \Omega_g, p \neq q} E_{pq}^{int}, \quad (3)$$

where \mathcal{H}_{pp} is the matrix element of the kinetic energy plus nuclear-electron attraction terms and $\mathcal{J}_{pp} = \langle pp|pp \rangle$ is the Coulomb interaction between two electrons with opposite spins at the spatial orbital p . The term E_{pq}^{int} contains the interaction energy between electrons in different spatial orbitals p , and q ,

$$E_{pq}^{int} = (n_q n_p - \Delta_{qp}) (2\mathcal{J}_{pq} - \mathcal{K}_{pq}) + \Pi_{qp} \mathcal{L}_{pq} \quad (4)$$

where $\mathcal{J}_{pq} = \langle pq|pq \rangle$ and $\mathcal{K}_{pq} = \langle pq|qp \rangle$ are the direct and exchange integrals, respectively and $\mathcal{L}_{pq} = \langle pp|qq \rangle$ is the exchange and time-inversion integral.²⁹ Matrices Δ and Π are auxiliary matrices proposed³⁰ to reconstruct the 2-RDM in terms of the NO occupancies. The diagonal elements of these matrices are $\Delta_{pp} = n_p^2$ and $\Pi_{pp} = n_p$. The off-diagonal elements of Δ and Π determine the different implementation of the PNOF i ($i = 1 - 6$) series. In particular, PNOF5 and PNOF6 differ on the treatment of the interaction between electrons on different pairs.

In PNOF5, when orbitals p and q belong to the same subspace Ω_g , the off-diagonal elements of Δ and Π are $\Delta_{pq} = n_q n_p$ and

$$\Pi_{pq} = \begin{cases} -\sqrt{n_q n_p}, & p = g \text{ or } q = g \\ \sqrt{n_q n_p}, & p, q > F, \end{cases} \quad (5)$$

respectively, and they vanish when p and q belong to different subspaces. Consequently, the second term of Eq. 2 becomes

$$\sum_{f \neq g} \sum_{p \in \Omega_f} \sum_{q \in \Omega_g} E_{pq}^{int} (\text{PNOF5}) = n_q n_p (2\mathcal{J}_{pq} - \mathcal{K}_{pq}). \quad (6)$$

The expression above indicates that the interaction between electrons in different pairs is treated at the mean-field level. Therefore, PNOF5 lacks correlation between electrons in different pairs. In contrast, the PNOF6 Δ_{pq} and Π_{pq} matrices (when p and q belong to different subspaces these matrices do not vanish) include terms that account for interpair electron correlation. The off-diagonal elements Δ_{pq} and Π_{pq} in PNOF6 read as

Δ_{qp}	Π_{qp}	Orbitals
$e^{-2S} h_q h_p$	$-e^{-S} (h_q h_p)^{\frac{1}{2}}$	$q \leq F, p \leq F$
$\frac{\gamma_q \gamma_p}{S_\gamma}$	$-\Pi_{qp}^\gamma$	$q \leq F, p > F$
$e^{-2S} n_q n_p$	$e^{-S} (n_q n_p)^{\frac{1}{2}}$	$q > F, p \leq F$
		$q > F, p > F$

(7)

where h_p is the hole ($1 - n_p$) in the spatial orbital p and S , γ_p , S_γ , and Π^γ are defined as

$$S = \sum_{q=1}^F h_q, \quad \alpha_p = \begin{cases} e^{-S} h_p, & p \leq F \\ e^{-S} n_p, & p > F \end{cases}$$

$$S_\alpha = \sum_{q=1}^F \alpha_q, \quad \gamma_p = n_p h_p + \alpha_p^2 - \alpha_p S_\alpha$$

$$S_\gamma = \sum_{q=1}^F \gamma_q, \quad \Pi_{qp}^\gamma = \left(n_q h_p + \frac{\gamma_q \gamma_p}{S_\gamma} \right)^{\frac{1}{2}} \left(h_q n_p + \frac{\gamma_q \gamma_p}{S_\gamma} \right)^{\frac{1}{2}} \quad (8)$$

Recently, PNOF5 has been proved equivalent to an antisymmetrized product of strongly orthogonal geminals (APSG).^{31,32} Conversely, PNOF6 is not related to geminal theories but it keeps the orbital-pairing scheme, Eq. 1. In this

work we have used the $N_c = 1$ version of the functionals. That is, each orbital subspace contains two spatial orbitals and then only N spatial orbitals are correlated. In this sense, both functionals take into account most of the nondynamic correlation effects, but while PNOF5 includes only intrapair correlation, PNOF6 incorporates also the interpair correlation, through Δ and Π matrices defined in Eq. 7 (see Eq.4)

B. Local Spin And Electron Delocalization

Local spins can be obtained by decomposing the expectation value of the total spin square operator $\langle \hat{S}^2 \rangle$ into atomic or fragment contributions as

$$\langle \hat{S}^2 \rangle = \sum_A \langle \hat{S}^2 \rangle_A + \sum_{A \neq B} \langle \hat{S}^2 \rangle_{AB}, \quad (9)$$

where $\langle \hat{S}^2 \rangle_A$ is the local spin on fragment A and $\langle \hat{S}^2 \rangle_{AB}$ accounts for the coupling between spins on fragments A and B . Recently some of us have presented a general formulation of the local spin that fulfills a set of physical constraints.^{24,25} For singlet systems, the formulation reads as

$$\begin{aligned} \langle \hat{S}^2 \rangle_A = & \frac{3}{4} \left(2 \text{Tr}({}^1\mathbf{D}\mathbf{S}^A) - \text{Tr}({}^1\mathbf{D}\mathbf{S}^{A1}\mathbf{D}) \right) \\ & + \frac{1}{2} \sum_{ijkl} \Gamma_{ij;kl} S_{ki}^A S_{lj}^A - \frac{1}{2} \sum_{ijkl} \Gamma_{ij;kl} S_{li}^A S_{kj}^A \end{aligned} \quad (10)$$

and

$$\langle \hat{S}^2 \rangle_{AB} = \frac{1}{2} \sum_{ijkl} \Gamma_{ij;kl} S_{ki}^A S_{lj}^B - \frac{1}{2} \sum_{ijkl} \Gamma_{ij;kl} S_{li}^A S_{kj}^B \quad (11)$$

where ${}^1\mathbf{D}$, Γ , and \mathbf{S}^A are the spinless 1-RDM, the spinless cumulant of the 2-RDM, and the fragment orbital overlap matrix.²⁴ The correct description of local spins has been recently put forward as a stringent condition to test natural-orbital based cumulant matrix (or 2-RDM) approximations,²⁶ and has been used to characterize and quantify the diradical and triradical character of molecules.^{33,34} In this work, we will use the local spin analysis to study the effect of the interpair electron correlation in PNOF5 and PNOF6 on the spin coupling of electrons located at different atoms.

The calculation of electron delocalization among different fragments can be performed through the NO-weighted overlap multiplications involving the different fragments. This is commonly known as Giambiagi's multicenter index³⁵ and its expression reads³⁶

$$I_{ABCD} = \sum_{ijkl} n_i n_j n_k n_l S_{ij}^A S_{jk}^B S_{kl}^C S_{li}^D \quad (12)$$

The quantity has been successfully used to account for several multicenter delocalization phenomena including multicenter bonding,³⁷ conjugation effects³⁸ and aromaticity.^{39,40}

III. COMPUTATIONAL DETAILS

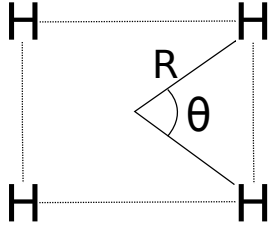
In this work we have computed the D_{4h}/D_{2h} PES of H_4 employing the following methods: Hartree-Fock (HF), CC singles and doubles (CCSD), CCSD with perturbative estimation of triple excitations (CCSD(T)), complete active space self-consistent field CASSCF (with a 4 electrons in 4 orbitals active space), PNOF5, PNOF6 and full configuration interaction (FCI). This benchmark data set includes methods that mostly include dynamic correlation effects (CCSD and CCSD(T)) or nondynamic correlation effects (CASSCF) and will be used as benchmark references to measure the amount of dynamic and nondynamic correlation effects included in PNOF5 and PNOF6.

All calculations based on wave function methods have been performed with the Gaussian03⁴¹ set of programs except those at the FCI level that were performed with a modified version of the program of Knowles and Handy.^{42,43} NOF calculations have been carried out using DoNOF program. The matrix elements of the kinetic energy, the nuclear-electron attraction energies, and the one- and two-electron integrals needed to perform the PNOF calculations have been obtained from GAMESS.^{44,45} The correlation-consistent aug-cc-pVDZ⁴⁶ basis set has been employed for all the calculations. The local spin analysis has been performed using DMN⁴⁷ to compute the 2-RDM and APOST-3D⁴⁸ to calculate the local spins using the topological fuzzy Voronoi cells to define the atomic regions.⁴⁹

IV. RESULTS

The PES of H_4 is characterized using two parameters, R and θ (see Fig. 1). The former, controls the distance between each H atom and the center of mass while the latter measures the angle formed by two neighbor H atoms and the center of mass (see Fig. 1). At $\theta = 90^\circ$, the system possesses D_{4h} symmetry and two configurations with symmetries $a_g^2 b_{3u}^2$ and $a_g^2 b_{3u}^2$ become degenerate. By modifying θ one can control the degree of symmetry distortion with respect to the D_{4h} ($\theta = 90^\circ$) structure, thus modulating the multireference character (and hence the nondynamic correlation) of the system. In this sense, the H_4 PES represents a challenging system for most electronic structure methods as it combines nondynamic correlation and dynamic correlation effects.

The relative energies with respect to the minimum energy at $\theta = 70^\circ$ for each method of the H_4 model keeping R constant for different distances and modifying θ are shown in Fig. 2. The system is symmetric at $\theta = 90^\circ$ and it is described by two degenerate configurations, which correspond to the minimum HF solutions at $\theta < 90^\circ$ and $\theta > 90^\circ$, respectively. The FCI curve has an energy maximum at $\theta = 90^\circ$ and the energy curve is smooth along the entire range of angles. The energy needed to change from $\theta = 70^\circ$ to the D_{4h} geometry decreases gradually as the radius R increases until the PES

FIG. 1. D_{4h}/D_{2h} H_4 model.

becomes considerably flat. The CASSCF curves show the right qualitative features, *i.e.*, a maximum at $\theta = 90^\circ$ and a smooth transition from $\theta = 70^\circ$ to $\theta = 110^\circ$. However, due to missing dynamic correlation energy that becomes important at the $\theta \gg 90^\circ$ and $\theta \ll 90^\circ$ regions, CASSCF relative values are downshifted to lower energies.

At $\theta = 90^\circ$ two configurations become degenerate and the HF solution presents symmetry-breaking artifacts that result in a maximum cusp in the energy profile.¹⁷ Therefore, it is only natural that most post-HF single-reference methods based on the RHF reference also fail to qualitatively describe this PES. Although at small R values CCSD and CCSD(T) mimic the FCI PES, as the radius R increases first CCSD(T) (at $R = 0.80\text{\AA}$) and then CCSD (at $R = 1.20\text{\AA}$) break down and show a cusp of the PES at $\theta = 90^\circ$, which —unlike the HF cusp— is a local minimum with respect to θ . Since CASSCF with a (4,4) active space shows a qualitative right result and dynamic-correlation-including methods produce an artifact at $\theta = 90^\circ$, one attributes this feature to the lack of nondynamic correlation effects. Consequently, at short values of R and for the θ values considered, the CC results are in perfect agreement with FCI.

PNOF5 —a nondynamic-correlation-including method— shows a maximum cusp at $\theta = 90^\circ$, like VCC,¹³ OQVCCD and OQVCCD(T),²⁰ and the lately introduced CCD0 and CCSD0, which are single-reference CC variants that exclude certain excitations.² This result suggests that PNOF5 is missing some nondynamic correlation and it is only this fraction of nondynamic correlation that is responsible for the spurious cusp.

On the other hand, PNOF6 which —at variance with PNOF5— includes interpair correlation, shows a smooth PES for $R \leq 1.5\text{\AA}$, suggesting that only interpair nondynamic correlation is actually needed to obtain a cusp-free, qualitatively correct description of the H_4 PES at values close to the minimum energy geometry. When $R = 1.70\text{\AA}$ and 1.90\AA , the PNOF6 solution is not perfectly smooth. This behavior is due to the crossing of two solutions of the PNOF6 equations as can be seen in Fig. 3. In this graphic, the minimum PNOF6 solution is showed in solid lines. One can see the crossing of two solutions at $\theta \simeq 80^\circ, 90^\circ$, and 100° for $R = 1.70\text{\AA}$ and at $\theta \simeq 70^\circ, 90^\circ$, and 110° for $R = 1.90\text{\AA}$. At large R only one solution (labeled Sol. 2 in Fig. 3) of the PNOF6 equations is found, there is no longer a crossing and the PES smoothness is recovered, the shape of PNOF6 and FCI relative energies

TABLE I. Relative energies (kcal/mol) as the difference between the absolute energies at $\theta = 90^\circ$ and $\theta = 70^\circ$ for different values of $R(\text{\AA})$.

Method	R=0.80	R=1.00	R=1.20	R=1.40	R=1.60	R=1.80
FCI	68.75	61.54	48.92	35.58	23.79	14.72
HF	99.15	99.43	93.38	85.20	76.59	68.33
CASSCF	66.61	58.19	45.44	32.68	21.66	13.27
PNOF5	87.63	78.67	61.88	43.67	27.94	16.47
PNOF6	74.19	68.98	57.74	44.48	30.68	18.17

being almost indistinguishable.

Table I gathers the relative energies at $\theta = 70^\circ$ with respect to the energy at $\theta = 90^\circ$. For $R = 0.8\text{\AA}$, $R = 1.00\text{\AA}$, and $R = 1.20\text{\AA}$ PNOF6 improves PNOF5 (as to compared to FCI) by 13.44, 9.69 and 4.14 kcal/mol, respectively. At larger values of R , PNOF5 improves over PNOF6 but the difference between them does not exceed 3 kcal/mol. CASSCF results are closer to FCI than PNOF6 for all the distances. The difference attains its maximum at $R = 1.20\text{\AA}$, in which CASSCF is 12.29 kcal/mol closer to FCI than PNOF6. These deviations put forward the current limits of PNOF6 to fully account for correlation effects.

In table II we collect FCI, PNOF5, and PNOF6 absolute energies for $R = 0.80\text{\AA}$, 1.20\AA , and 1.70\AA . PNOF5 energies are in all cases closer to FCI than PNOF6. This is due to the repulsive electron-electron interpair correlation energy term that is included in the PNOF6 functional. PNOF6 improves qualitatively the shape of the PES, provides good relative energies at the price of higher absolute energies.

APSG, which is the antisymmetric wavefunction behind PNOF5,³¹ has been shown to also exhibit this spurious maximum cusp at $\theta = 90^\circ$.²³ The failure of APSG has been attributed to the localized nature of its orbitals and the wrong account of spin coupling. Szabados and coworkers²² have demonstrated that APSG using delocalized orbitals, which correspond to a solution of the ASPG equations, eliminates the cusp. In Fig. 4 we plot the orbitals that arise from PNOF6 and PNOF5 at $R = 1.0\text{\AA}$ and $\theta = 90^\circ$. PNOF5 NO are localized on $H - H$ bonds and each bonding orbital is coupled with its antibonding counterpart. At this value of θ , the same picture with the orbitals *horizontally* localized is equivalent. On the other hand, the PNOF6 NO present the expected delocalized character and mimic the canonic orbitals obtained in a HF calculation. Importantly, both solutions showed in Fig. 3 for $R = 1.70\text{\AA}$ and 1.90\AA present delocalized orbitals. Unlike PNOF5, PNOF6 equations do not lead to a stationary solution that corresponds to a set of localized orbitals.

The inclusion of interpair correlation also affects the occupation numbers of the corresponding NO (see table III). For small values of R at the CASSCF level, the a_g orbital remains almost doubly occupied along the PES. The b_{2u} is doubly occupied for $\theta \ll 90^\circ$ and there is a smooth transition from these structures to the $\theta \gg 90^\circ$ ones in which the doubly occupied orbital is the b_{3u} . At $\theta = 90^\circ$ both orbitals become

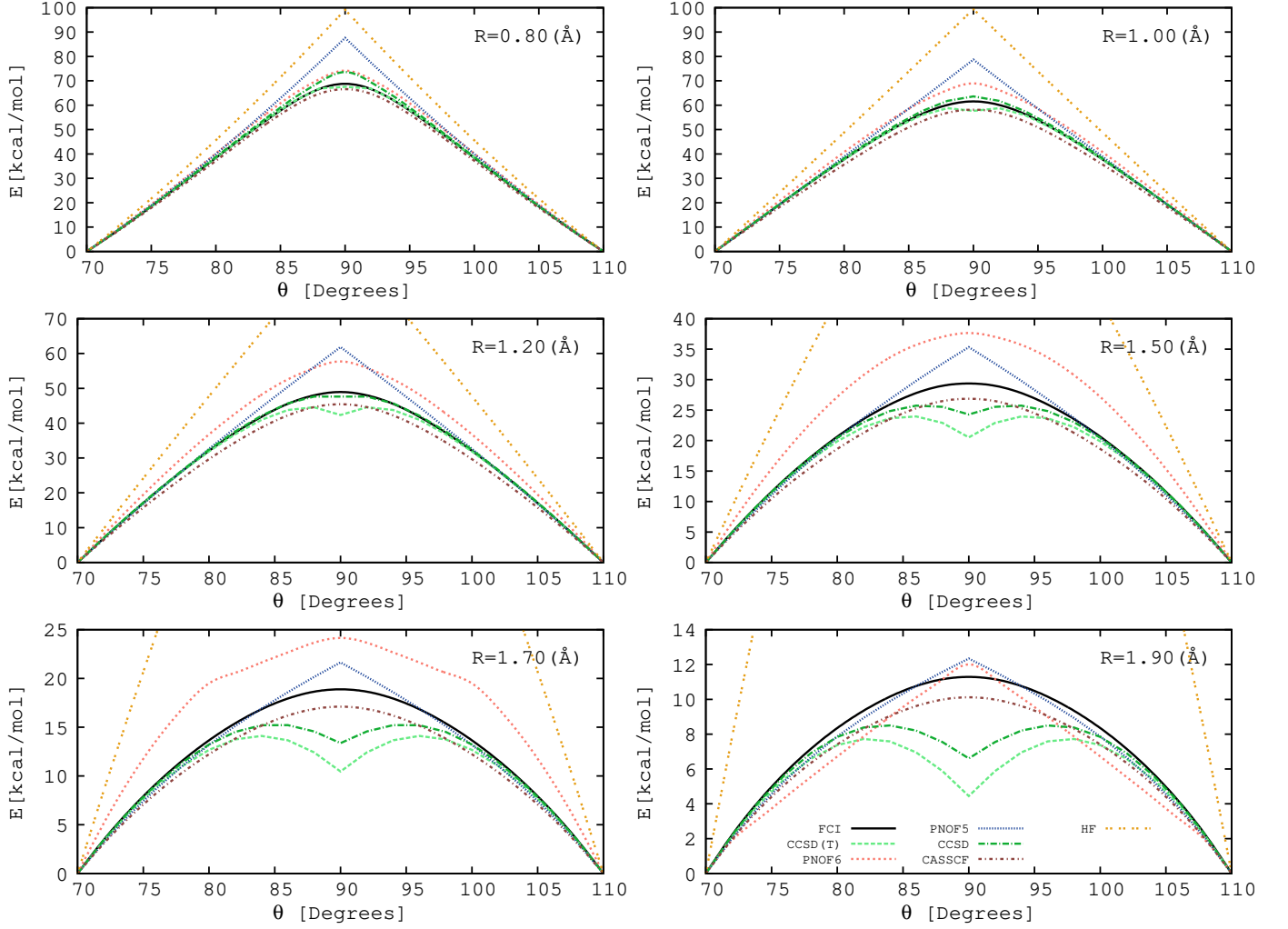


FIG. 2. Relative energies in kcal/mol with respect to the lowest energy found for each method $\theta = 70^\circ$, along the D_{2h}/D_{4h} PES of H_4 .

TABLE II. FCI, PNOF5, and PNOF6 H_4 absolute energies in a.u. for different values of θ and R

θ°	$R = 0.80 \text{ \AA}$			$R = 1.20 \text{ \AA}$			$R = 1.70 \text{ \AA}$		
	FCI	PNOF5	PNOF6	FCI	PNOF5	PNOF6	FCI	PNOF5	PNOF6
70	-2.20639	-2.16625	-2.14177	-2.14307	-2.11972	-2.06829	-2.04310	-2.03505	-1.93271
72	-2.19498	-2.15467	-2.12979	-2.13184	-2.10876	-2.05554	-2.03759	-2.02993	-1.92448
74	-2.18305	-2.14247	-2.11728	-2.12105	-2.09810	-2.04323	-2.03271	-2.02533	-1.91722
76	-2.17071	-2.12970	-2.10437	-2.11077	-2.08772	-2.03143	-2.02840	-2.02118	-1.91097
78	-2.15805	-2.11639	-2.09113	-2.10104	-2.07760	-2.02022	-2.02462	-2.01744	-1.90572
80	-2.14523	-2.10259	-2.07771	-2.09195	-2.06773	-2.00970	-2.02135	-2.01404	-1.90165
82	-2.13244	-2.08832	-2.06428	-2.08364	-2.05809	-2.00005	-2.01855	-2.01094	-1.89992
84	-2.12005	-2.07358	-2.05117	-2.07635	-2.04864	-1.99151	-2.01626	-2.00809	-1.89823
86	-2.10881	-2.05839	-2.03902	-2.07046	-2.03936	-1.98445	-2.01451	-2.00543	-1.89659
88	-2.10023	-2.04273	-2.02916	-2.06652	-2.03019	-1.97926	-2.01339	-2.00294	-1.89499
90	-2.09683	-2.02660	-2.02354	-2.06512	-2.02111	-1.97628	-2.01300	-2.00055	-1.89423

degenerate in terms of occupancies. The PNOF5 bonding orbitals are almost doubly occupied along the PES while the antibonding ones remain almost unoccupied. No degeneracy is observed in this case. By including interpair electron correlation, PNOF6 NO and occupancies qualitatively mimic

the CASSCF ones. It is worth noting that at $\theta = 90^\circ$ the b_{3u} and b_{2u} do not have exactly the same occupancy for most of the values of R shown in Fig. III. This might indicate that the interpair description is not fully recovered by PNOF6. The second solution shown in Fig. 3 as PNOF6(sol. 2), that

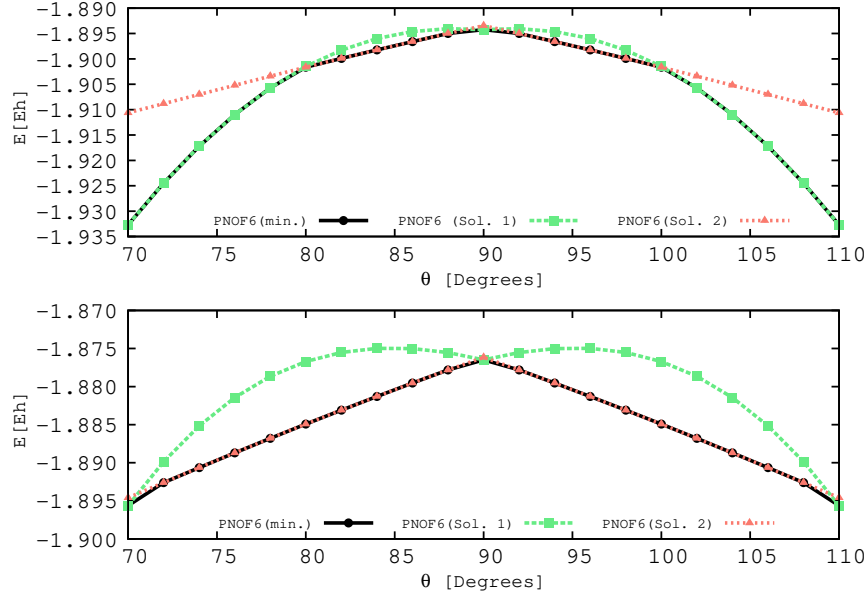


FIG. 3. Absolute PNOF6 energies in a.u. for $R = 1.70\text{\AA}$ (top) and $R = 1.90\text{\AA}$ (bottom). PNOF6(Sol. 1) and PNOF6(Sol. 2) stand for the two solutions that show a crossing and PNOF6(min.) stand for the minimum energy solution of each value of θ .

TABLE III. CASSCF(4,4), PNOF5, and PNOF6 NO occupation numbers at $\theta = 90^\circ$ for different values of R .

$R(\text{\AA})$	n_1	n_2	n_3	n_4
CASSCF				
0.80	1.939	1.000	1.000	0.061
1.00	1.882	1.000	1.000	0.118
1.20	1.795	1.000	1.000	0.205
1.50	1.604	1.000	1.000	0.396
1.70	1.458	1.000	1.000	0.542
1.90	1.327	1.000	1.000	0.673
20.00	1.000	1.000	1.000	1.000
PNOF5				
0.80	1.923	1.921	0.079	0.077
1.00	1.835	1.835	0.165	0.165
1.20	1.704	1.704	0.296	0.296
1.50	1.472	1.471	0.529	0.528
1.70	1.335	1.335	0.665	0.666
1.90	1.229	1.229	0.771	0.771
20.00	1.000	1.000	1.000	1.000
PNOF6				
0.80	1.971	1.185	0.815	0.029
1.00	1.942	1.197	0.803	0.058
1.20	1.894	1.191	0.809	0.106
1.50	1.771	1.150	0.850	0.230
1.70	1.645	1.110	0.891	0.355
1.90	1.495	1.068	0.932	0.505
20.00	1.000	1.000	1.000	1.000

becomes the minimum energy solution for certain values of θ when $R = 1.70\text{\AA}$ and 1.90\AA and is the minimum solution found for larger values of R , presents perfect degeneracy in terms of occupation numbers of the b_{3u} and b_{2u} orbitals for all values of θ and R .

The wrong coupling between spins located in different centers of the molecule is one of the causes for the failure

of singlet-couplet geminal approaches to describe the H_4 system. Jeszenszki *et al.* have used the local spin analysis to show that the inclusion of triplet components in geminals improves the APSG results but spin contamination appears when the triplet component in the geminal becomes important. The local spin value of one H atom of the H_4 system is shown in Fig. 5. As the system approaches the D_{4h} symmetry, there is an increase of the diradical character of the system and

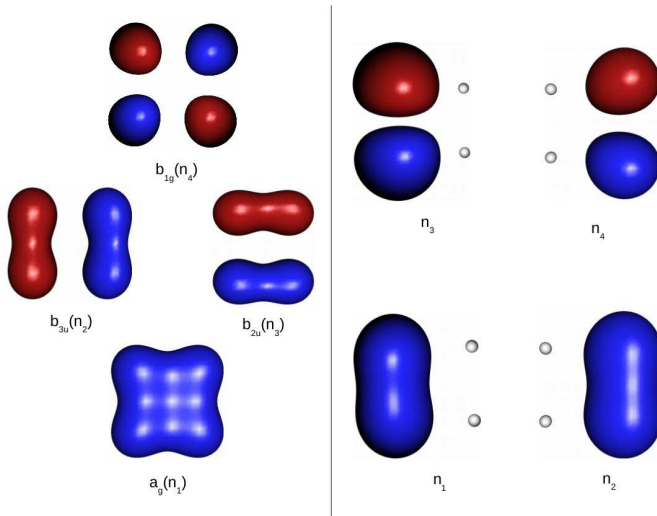


FIG. 4. PNOF6 (left), and PNOF5 (right) natural orbitals of H_4 for $R = 1.0 \text{ Å}$ and $\theta = 90^\circ$

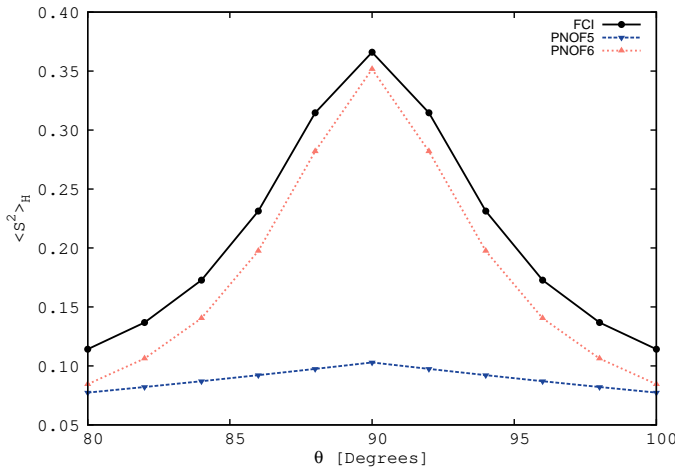


FIG. 5. Local spin values of one of the H atom of H_4 at $R = 0.80 \text{ Å}$ with respect to angle θ .

the local spin on atom H grows. PNOF5 cannot reproduce this trend and the local spin remains almost constant along the PES, while PNOF6 local spin values in H_4 are in good agreement with the FCI results.

Finally, let us examine the multicenter delocalization in the D_{2h} to D_{4h} transition. Fig. 6 shows that PNOF6 values closely follow the FCI ones and give a maximum electron delocalization in the D_{4h} structures, whereas PNOF5 shows a rather constant profile, clearly indicating its inability to delocalize the electron density along the H_4 skeleton.

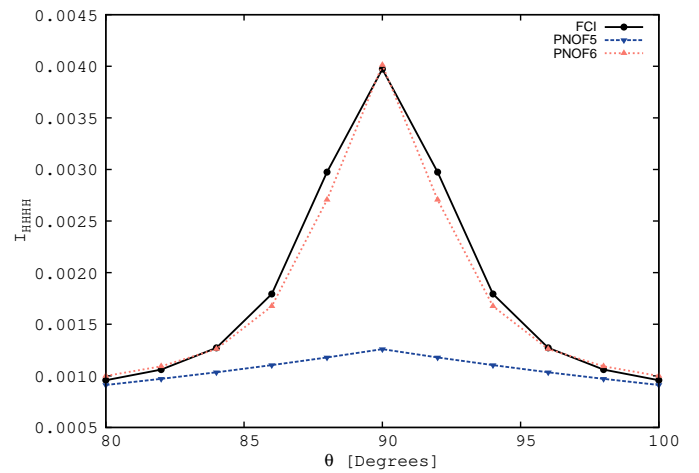


FIG. 6. Multicenter Giambiagi indices, Eq. 12, along the $D_{2h} - D_{4h}$ transition for $R = 0.80 \text{ Å}$ performed with PNOF5, PNOF6 and FCI natural orbitals.

V. CONCLUSIONS

The PES of the planar D_{4h}/D_{2h} H_4 model has been computed at several levels of theory. Single-reference methods show a spurious cusp at the D_{4h} structure that thus far was attributed to nondynamic correlation. PNOF5 (which affords a correct description of molecular dissociation and other intrapair nondynamic correlation effects) also shows a spurious cusp at D_{4h} , whereas PNOF6 provides a qualitatively correct description of this phenomenon.

Since PNOF5 and PNOF6 mainly differ from each other by the inclusion of interpair correlation, the factors responsible for the spurious description of the D_{4h}/D_{2h} H_4 PES can be narrowed down to missing *interpair* nondynamic correlation effects. Indeed, the inclusion of interpair correlation in the pairing-orbital NOFT ansatz is key to recover the delocalized orbitals picture, remove the spurious cusp in the PES and properly account for the coupling between the spins located at different centers. On the other hand, inclusion of more terms to fully account for electron correlation seems to be needed to recover the smoothness of the curves at $R = 1.70 \text{ Å}$ and 1.90 Å , to obtain quantitative results, and to recover the important correlation effects that separate PNOF6 results from FCI. We hope that this study will shed light on the effect of interpair electron correlation and pave the way to the development of new electronic structure methods within NOFT or methods based on geminal expansion of the wave function. Research in this direction is underway in our laboratory.

ACKNOWLEDGMENTS

This research has been funded by the MINECO projects CTQ2012-38496-C05-01, CTQ2012-38496-C05-04 and CTQ2014-52525-P and the Basque Country Consolidated

Group Project No. IT588-13. We are grateful for the computational resources granted at the MareNostrum computer of the Barcelona Supercomputing Center and technical and human support provided by SGI/IZO-SGIker UPV/EHU.

- ¹A. D. Becke, *J. Chem. Phys.* **140**, 18A301 (2014).
- ²I. W. Bulik, T. M. Henderson, and G. E. Scuseria, *J. Chem. Theory Comput.* (2015), 10.1021/acs.jctc.5b00422.
- ³T. L. Gilbert, *Phys. Rev. B* **12**, 2111 (1975).
- ⁴M. Piris, *Adv. Chem. Phys.* **134**, 387 (2007).
- ⁵K. Pernal and K. J. H. Giesbertz, (DOI:10.1007/128_2015_624), (and references therein).
- ⁶E. V. Ludeña, F. J. Torres, and C. Costa, *J. Mod. Phys.* **04**, 391 (2013).
- ⁷M. Piris, *Int. J. Quant. Chem.* **113**, 620 (2013), (and references therein).
- ⁸M. Piris and J. Ugalde, *Int. J. Quant. Chem.* **114**, 1169 (2014).
- ⁹M. Piris, X. Lopez, F. Ruipérez, J. M. Matxain, and J. M. Ugalde, *J. Chem. Phys.* **134**, 164102 (2011).
- ¹⁰M. Piris, *J. Chem. Phys.* **141**, 044107 (2014).
- ¹¹J. M. Matxain, M. Piris, F. Ruipérez, X. Lopez, and J. M. Ugalde, *Phys. Chem. Chem. Phys.* **13**, 20129 (2011).
- ¹²J. B. Robinson and P. J. Knowles, *J. Chem. Phys.* **137**, 054301 (2012).
- ¹³T. V. Voorhis and M. Head-Gordon, *J. Chem. Phys.* **113**, 8873 (2000).
- ¹⁴K. Jankowski and K. Kowalski, *J. Chem. Phys.* **110**, 9345 (1999).
- ¹⁵K. Jankowski and K. Kowalski, *J. Chem. Phys.* **110**, 3714 (1999).
- ¹⁶K. Kowalski and K. Jankowski, *Phys. Rev. Lett.* **81**, 1195 (1998).
- ¹⁷K. Kowalski and K. Jankowski, *Chem. Phys. Lett.* **290**, 180 (1998).
- ¹⁸J. Paldus, P. Piecuch, L. Pylypow, and B. Jeziorski, *Phys. Rev. A* **47**, 2738 (1993).
- ¹⁹J. B. Robinson and P. J. Knowles, *J. Chem. Phys.* **136**, 054114 (2012).
- ²⁰J. B. Robinson and P. J. Knowles, *J. Chem. Theory Comput.* **8**, 2653 (2012).
- ²¹A. M. Sand and D. A. Mazziotti, *Comp. Theor. Chem.* **1003**, 44 (2013).
- ²²P. Jeszenszki, V. A. Rassolov, P. R. Surján, and Á. Szabados, *Molec. Phys.* **113**, 249 (2015).
- ²³V. A. Rassolov and F. Xu, *J. Chem. Phys.* **127**, 044104 (2007).
- ²⁴E. Ramos-Cordoba, E. Matito, I. Mayer, and P. Salvador, *J. Chem. Theory Comput.* **8**, 1270 (2012).
- ²⁵E. Ramos-Cordoba, E. Matito, P. Salvador, and I. Mayer, *Phys. Chem. Chem. Phys.* **14**, 15291 (2012).
- ²⁶E. Ramos-Cordoba, P. Salvador, M. Piris, and E. Matito, *J. Chem. Phys.* **141**, 234101 (2014).
- ²⁷M. Piris, J. M. Matxain, and X. Lopez, *J. Chem. Phys.* **139**, 234109 (2013).
- ²⁸X. Lopez, M. Piris, F. Ruipérez, and J. M. Ugalde, *J. Phys. Chem. A* **119**, 6981 (2015).
- ²⁹M. Piris, *J. Math. Chem.* **25**, 47 (1999).
- ³⁰M. Piris, *Int. J. Quantum Chem.* **106**, 1093 (2006).
- ³¹K. Pernal, *Comp. Theor. Chem.* **1003**, 127 (2013).
- ³²M. Piris, *J. Chem. Phys.* **139**, 064111 (2013).
- ³³E. Ramos-Cordoba and P. Salvador, *J. Chem. Theory Comput.* **10**, 634 (2014).
- ³⁴E. Ramos-Cordoba and P. Salvador, *Phys. Chem. Chem. Phys.* **16**, 9565 (2014).
- ³⁵M. Giambiagi, M. Giambiagi, and K. Mundim, *Struct. Chem.* **1**, 423 (1990).
- ³⁶J. Cioslowski, E. Matito, and M. Solà, *J. Phys. Chem. A* **111**, 6521 (2007).
- ³⁷F. Feixas, M. Solà, J. M. Barroso, J. M. Ugalde, and E. Matito, *J. Chem. Theory Comput.* **10**, 3055 (2014).
- ³⁸F. Feixas, E. Matito, J. Poater, and M. Solà, *J. Phys. Chem. A* **115**, 13104 (2011).
- ³⁹M. Giambiagi, M. S. d. Giambiagi, C. D. dos Santos Silva, and A. P. da Figueiredo, *Phys. Chem. Chem. Phys.* **2**, 3381 (2000).
- ⁴⁰F. Feixas, E. Matito, J. Poater, and M. Solà, *Chem. Soc. Rev.* **44**, 6434 (2015).
- ⁴¹M. J. Frisch, "Gaussian 03, revision c. 02," (2003), Gaussian, Inc., Pittsburgh, PA, 2003.
- ⁴²P. J. Knowles and N. C. Handy, *Chem. Phys. Lett.* **111**, 315 (1984).
- ⁴³P. J. Knowles and N. C. Handy, *Comp. Phys. Com.* **54**, 75 (1989).
- ⁴⁴M. W. Schmidt, K. K. Baldrige, J. A. Boatz, S. T. Elbert, M. S. Gordon, J. H. Jensen, S. Koseki, N. Matsunaga, K. A. Nguyen, S. Su, T. L. Windus, M. Dupuis, and J. A. Montgomery, *J. Comput. Chem.* **14**, 1347 (1993).
- ⁴⁵M. S. Gordon and M. W. Schmidt, in *Theory and Applications of Computational Chemistry*, edited by C. E. Dykstra, G. Frenking, K. S. Kim, and G. E. Scuseria (Elsevier, 2005) pp. 1167–1189.
- ⁴⁶T. H. Dunning Jr, *J. Chem. Phys.* **90**, 1007 (1989).
- ⁴⁷E. Matito and F. Feixas, "DMN program," (2009), University of Girona (Spain) and University of Szczecin (Poland).
- ⁴⁸P. Salvador and E. Ramos-Cordoba, "Apost-3d program," (2012), Universitat de Girona (Spain).
- ⁴⁹P. Salvador and E. Ramos-Cordoba, *J. Chem. Phys.* **139**, 071103 (2013).